Neutron Drops and Skyrme Energy-Density Functionals

B. S. Pudliner,[1] A. Smerzi,[1,2] J. Carlson,[3] V. R. Pandharipande,[1] Steven C. Pieper,[4] and D. G. Ravenhall[1]
[1]*Department of Physics, University of Illinois, Urbana, Illinois 61801-3080*
[2]*Laboratorio Nazionale del Sud, Istituto Nazionale di Fisica Nucleare, v Andrea Doria, 95125 Catania, Italy*
[3]*Theoretical Division, Los Alamos National Laboratory, Los Alamos, New Mexico 87545*
[4]*Physics Division, Argonne National Laboratory, Argonne, Illinois 60439-4843*
(Received 5 September 1995)

The $J^\pi = 0^+$ ground state of a drop of 8 neutrons and the lowest $1/2^-$ and $3/2^-$ states of 7-neutron drops, all in an external well, are computed accurately with variational and Green's function Monte Carlo methods for a Hamiltonian containing the Argonne v_{18} two-nucleon and Urbana IX three-nucleon potentials. These states are also calculated using Skyrme-type energy-density functionals. Commonly used functionals overestimate the central density of these drops and the spin-orbit splitting of 7-neutron drops. Improvements in the functionals are suggested.

PACS numbers: 21.65.+f, 21.10.Dr, 21.60.Ka, 26.60.+c

Properties of neutron matter are vitally important in determining the structure of neutron stars [1], and have a strong bearing on the energies of neutron-rich nuclei, and on the r-process in nucleosynthesis [2]. It is impossible to extrapolate available data on nuclei to the region of neutron matter with sufficient precision using effective interactions. Different effective interactions that fit the energies of laboratory nuclei rather well predict very different equations of state for neutron matter [1]. In contrast, it appears that modern calculations of neutron matter based on realistic models of nuclear forces are much more consistent with each other at densities $\rho \lesssim 0.16$ fm^{-3} [3], and therefore are presumably more reliable. The two-nucleon interaction in these realistic models is better determined from the scattering data in isospin $T = 1$ states than that in $T = 0$, and the uncertainties coming from three-nucleon forces and relativistic effects are also much smaller in neutron than in nuclear matter. Calculations of uniform neutron matter have provided important constraints on Skyrme-type effective interactions used to study neutron-rich systems. They do not, however, provide information on the strength of the spin-orbit interaction, nor on other terms sensitive to density gradients, both of which may affect significantly the predicted properties of drip-line nuclei and of neutron-star matter.

Ab initio calculations of finite nuclei, based on realistic models of nuclear forces, can provide the necessary additional information, but they are more challenging. Recently [4] the energies of nuclei with $A \leq 6$ have been calculated essentially exactly with the Green's function Monte Carlo (GFMC) method. Cluster variational Monte Carlo (CVMC) calculations have also been used to study ^{16}O [5] and the spin-orbit splitting (SOS) in ^{15}N [6]. In this Letter we report GFMC and CVMC calculations of states of seven and eight neutrons bound in a weak external potential well using the new Argonne two-nucleon [7] and Urbana three-nucleon interactions used in Ref. [4]. These interactions accurately reproduce the available two-nucleon scattering data and binding energies of $A \leq 6$ nuclei. Neutron matter is not bound, therefore an external well ($V_{\rm ex}$) is necessary to hold the neutrons together. We have used a Woods-Saxon well with $V_0 = -20$ MeV, $R = 3$ fm, and $a = 0.65$ fm, chosen such that with it alone only the single-neutron $1s$ state is bound at -5.73 MeV, while the $1p$ and higher states are unbound. The investigated states of seven and eight neutrons are thus bound by both the well and the interaction between neutrons. We denote them by $^8n(J^\pi = 0^+)$ and $^7n(J^\pi = 1/2^-$ and $3/2^-)$.

The present variational Monte Carlo (VMC) and GFMC calculations are simpler than those for nuclei [4] because all nucleons are neutrons; they use the variational wave function

$$|\Psi_V\rangle = \left[S \prod_{i<j} (1 + U_{ij}) \right] \left[\prod_{i<j} f_c(r_{ij}) \right] |\Phi\rangle , \quad (1)$$

$$U_{ij} = u_\sigma(r_{ij})\, \sigma_i \cdot \sigma_j + u_t(r_{ij}) S_{ij} . \quad (2)$$

Here $S\Pi$ denotes a symmetrized product, S_{ij} is the tensor operator, $f_c(r_{ij})$ is the Jastrow correlation, and $|\Phi\rangle$ is an antisymmetric shell model wave function. The three-body correlations commonly used in nuclear Ψ_V are omitted because they have little effect on the energies of low-density neutron systems, and the two-body spin-orbit correlations are discussed later along with an improved Ψ_V. The radial wave functions of the s and p orbitals in Φ and the correlation functions f_c, u_σ, and u_t are determined variationally.

The GFMC calculations are carried out as described in Ref. [4] with a simpler Hamiltonian,

$$H = -\sum_i \frac{\hbar^2}{2m} \nabla_i^2 + \sum_i V_{\rm ex}(i) + \sum_{i<j} v_8'(ij) + \sum_{i<j<k} V_{ijk} , \quad (3)$$

where the v_8' does not contain L^2 or $(LS)^2$ terms; it equals the charge-symmetric part of the Argonne v_{18} interaction [7] in the $^1S_0$ and $^3P_{J=0,1,2}$ two-neutron states. The small

 0031-9007/96/76(14)/2416(4)$10.00

difference between the full v_{18} and v_8' is treated as a first-order perturbation, whose contribution to the calculated energies is <0.2 MeV.

The calculated transient energies,

$$E(\tau) = \langle \Psi_V | H e^{-(H-E_0)\tau} | \Psi_V \rangle / \langle \Psi_V | e^{-(H-E_0)\tau} | \Psi_V \rangle , \tag{4}$$

are shown in Fig. 1. The $E(\tau \to \infty)$ converges to the lowest eigenvalue of the chosen J^π. In Fermi systems, the statistical error in $E(\tau)$ increases with τ as configurations diffuse across nodal surfaces of the wave function [8] limiting our studies to $\tau < 0.04$ MeV^{-1}. The average values of $E(\tau)$ for $\tau = 0.032$, 0.036, and 0.04 MeV^{-1}, denoted by $\bar{E}$, are shown by horizontal lines in Fig. 1. The $E(\tau)$ of the $^8n(0^+)$ and $^7n(1/2^-)$ states do not have much τ dependence for $\tau > 0.015$ MeV^{-1}, suggesting that their $\bar{E}$ can be identified with the eigenvalues. In contrast, the $E(\tau)$ of the $^7n(3/2^-)$) state has more τ dependence. Consequently, the eigenvalue of the lowest $^7n(3/2^-)$ state could be a little below its $\bar{E}$ value. However, we will neglect that difference and regard it as our best estimate of the eigenvalue. The GFMC estimate of the density distribution of neutrons in the $^8n(0^+)$ drop is shown in Fig. 2. These results can be used to test the accuracy of the CVMC method and to further constrain the Skyrme-type energy-density functionals used to study neutron-rich nuclei and neutron-star crusts as discussed below.

The CVMC method and its modification for SOS are described in Refs. [5,6]. The present CVMC calculations are more accurate; they include contributions of all correlations and interactions up to five-body clusters. In contrast, in [5,6] contributions of only static correlations and interactions were calculated up to four-body clusters and the momentum-dependent terms were evaluated only at the two-body level. With the simpler Ψ_V given by Eq. (1), the one- to five-body cluster contributions to the energy of $^8n(0^+)$ state are, respectively, 12.9, -54.5, 11.1, -3.8, and 1.1 MeV, which sum to $-33.3(2)$ MeV. The $E(\tau = 0)$ is just the variational energy calculated to all orders without cluster expansion. Its value of $-33.7(1)$ MeV is very close to the CVMC result retaining up to five-body clusters. Even in this rather low-density system, the cluster expansion has a slow convergence, and it appears necessary to include five-body cluster contributions to reduce the truncation error to $<2\%$.

The simple Ψ_V [Eq. (1)] is not very accurate; the energy obtained with it is ~ 4 MeV (or $\sim 11\%$) too large. In CVMC we use the more general variational wave functions,

$$|\Psi_V'\rangle = \left[1 + \sum_{i<j<k} U_{ijk}\right] \left[S \prod_{i<j} (1 + U_{ij})\right] \times \left[1 + \sum_{i<j} u_{LS}(r_{ij}) L_{ij} (\sigma_i + \sigma_j)\right] \times \left[\prod_{i<j} f_c(r_{ij})\right] |\Phi\rangle , \tag{5}$$

where the three-body correlations, U_{ijk}, are of the kind used in Refs. [5,6], and as before the U_{ij} contains spin and tensor terms. The energies obtained with the Ψ_V' variational wave functions are, respectively, $-35.6(1)$, $-31.2(1)$, and $-29.7(1)$ MeV for the $^8n(0^+)$, $^7n(\frac{1}{2}^-)$, and $^7n(\frac{3}{2}^-)$ states. They are only $\sim 4\%$ above the GFMC energies $-37.6(3)$, $-32.3(2)$, and $-31.2(2)$ MeV. The CVMC calculations require about a factor of 25 less computer time than the GFMC, even allowing for the variational search, and it is possible to reduce the statistical error to a fraction of 1%. Much of the improvement in Ψ_V' comes from the spin-orbit correlations omitted in the

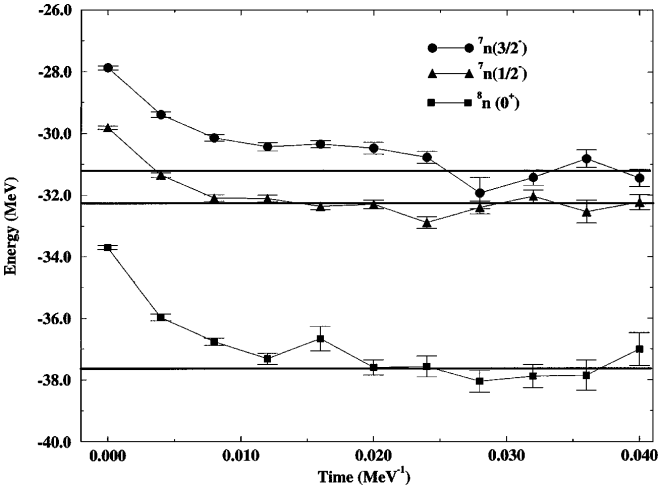

FIG. 1. The transient energy $E(\tau)$ for the GFMC calculations of $^8n(0^+)$ and $^7n(1/2^-$ and $3/2^-)$ as a function of the imaginary time τ.

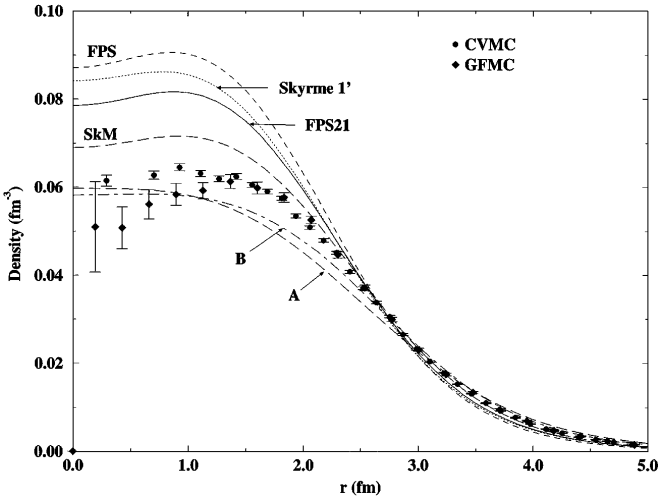

FIG. 2. Neutron density distribution for ^8n, according to methods described in the text. The curves labeled *A* and *B* come from modified versions of the effective interaction FPS21.

simpler Ψ_V. In the present GFMC calculations, the spin-orbit correlations are built in exactly via the propagation in imaginary time.

The contributions of the two-pion exchange part of the three-nucleon interaction, $V_{ijk}^{2\pi}$, to the GFMC energies of $^8n(0^+)$, $^7n(\frac{1}{2}^-$ and $\frac{3}{2}^-)$ are, respectively, 0.23, 0.13, and 0.13 MeV while those of the phenomenological V_{ijk}^{R} are 0.65, 0.42, and 0.59 with a sampling error of $\sim$0.08 MeV. In laboratory nuclei, these contributions are much larger, e.g., the total $\langle V_{ijk}\rangle$ is ~ -6.2 MeV in ^{6}Li [4] Their small values here are presumably due to the Pauli principle forbidding three neutrons to come close and the absence of the n-p $^3S_1 - ^3D_1$ coupled state through which the $V_{ijk}^{2\pi}$ gives a large negative contribution.

Fragmentation of the $p_{3/2}$ strength in ^{15}N results in the SOS of $p_{1/2}$ and $p_{3/2}$ quasihole states being $\sim$0.6 MeV larger than the observed splitting between the lowest $3/2^-$ and $1/2^-$ states in ^{15}N [6,9]. If W denotes the energy width of the fragmentation, the GFMC transient energies, $E(\tau)$, for $\tau \geq 1/W$ will include fragmentation effects. Since W is expected to be only a few MeV, it is very unlikely that the present $\bar{E}$ evaluated up to $\tau \sim 0.04$ has any fragmentation effects. The ^7n variational wave functions are constructed by removing an appropriate state from the $|\Phi\rangle$ and thus correspond to quasihole states. Presumably, they too do not contain any fragmentation effects. Hence, we identify the difference between the calculated energies of the $^7n(1/2^-)$ and $(3/2^-)$ states as the spin-orbit splitting. Its values are 1.1 ± 0.3 and 1.4 ± 0.1 MeV in the GFMC and CVMC calculations, respectively.

Four energy-density functionals (EDF) commonly used for astrophysical investigations, as discussed in Ref. [1], are (i) Skyrme 1′—Vautherin-Brink Skyrme model 1 [10] modified [11] to fit the neutron-matter $E(\rho)$ of Ref. [12]; (ii) SkM—Skyrme model M [13]; (iii) FPS and (iv) FPS-21 are generalized Skyrme models fitted approximately [14] and accurately [1] to the nuclear- and neutron-matter energies of Ref. [15]. These EDF's reproduce the ground-state energies of stable closed-shell nuclei rather accurately. The root mean square deviations $|\Delta E/E|$ between their prediction and experiment for ^{16}O, ^{40}Ca, ^{48}Ca, ^{56}Ni, ^{90}Zr, ^{114}Sn, ^{140}Ce, and ^{208}Pb are listed in Table I. This table also contains their predictions for the energy of the ^8n ground state and the ^7n and ^{15}N SOS. The results for the density distributions $\rho(r)$ of the $^8n(0^+)$ state are compared with the GFMC and CVMC $\rho(r)$ in Fig. 2.

In trying to learn from the departures of the EDF results for ^8n and ^7n from our benchmarks, we concentrate on the FPS21 effective interaction, since it gives the closest fit to the neutron-matter energies. Possible sources of difference include the fact that the neutron-matter energies used [15] date from an earlier period, whereas the benchmark results use newer interactions and more subtle computational techniques; also, and more importantly, the density-gradient terms in FPS21 are related to the effective-mass results [15] assuming a zero-range nucleon-nucleon interaction with no spin exchange. The latter simplification is common to all of the above EDF's and is not well justified. On the assumption that this is a contributor to the discrepancy, we have examined the effect of adding the term $\frac{1}{2}\alpha(\rho_n + \rho_p)^\beta(\nabla\rho_n - \nabla\rho_p)^2$ to the FPS21 (EDF). Such a term has little effect on $N \sim Z$ laboratory nuclei, but it can correct for the overbinding of $^8n(0^+)$, and also reduce the central neutron densities. We find that it cannot give good fits to these quantities simultaneously, however. For the two sets of coefficients $(\beta, \alpha) = (0, 150\ \text{MeV fm}^8)$ and $(2, 7 \times 10^4\ \text{MeV fm}^{14})$ the ground-state energies of ^8n are -39.6 and -40.2 MeV, respectively, and the neutron density distributions are shown as curves A and B in Fig. 2.

The present CVMC and GFMC results clearly indicate that the SOS predicted by the unadjusted Skyrme models for ^7n is too large, while it is good for ^{15}N. Relativistic mean-field models also predict a weaker spin-orbit potential in neutron-rich nuclei [16]. The neutron spin-orbit potential in these Skyrme models is of the form

$$V_{\ell s}^{(n)}(r) = W_{\ell s}\frac{1}{r}\frac{d}{dr}[\rho\,(r) + \rho_n(r)], \qquad (6)$$

TABLE I. Comparison of microscopic and Skyrme-model energies.

	^{8}n(0^+) (MeV)	^{7}n SOS (MeV)	Magic nuclei $\lvert\Delta E/E\rvert_{\text{rms}}\%$	^{15}N SOS[a] (MeV)	$W_{\ell s}$ (MeV^5)
GFMC	$-37.6(3)$	1.1(3)			
CVMC	$-35.5(1)$	1.4(1)	—	6.1[b]	
SkM	-47.4	3.0	1.1	6.3	130
FPS-21	-42.2	3.0	1.1	6.7	110
Skyrme 1′	-38.7	2.9	1.8	6.9	120
FPS	-32.5	3.5	1.2	6.7	110

[a]Experimental value 6.9 MeV deduced from Ref. [6].

[b]With Argonne v_{14}, Ref. [6].

obtained by Vautherin and Brink [10] assuming that it originates from two-nucleon interactions in the triplet-P state. Here $\rho(r) = \rho_n(r) + \rho_p(r)$ and $W_{\ell s}$ is a constant determined from the SOS in laboratory nuclei and listed in Table I. The form of this potential, proportional to a radial derivative of the densities, indicates that apart from other dependences the SOS obtained with a given EDF will depend on the nucleon central densities given by that model. The two modified versions of FPS21 just described, for the same value $W_{\ell s} = 110$ MeV used in Table I, each give a SOS in ^7n of 2.2 MeV. The reduction from the value of 3 MeV for unmodified FPS21 occurs because of the reduced central densities induced by the extra gradient term. The SOS in these modified models is still about double the value predicted by CVMC and GFMC, however.

As discussed in Ref. [6], more than half the SOS in ^{15}N comes from three-nucleon contributions involving either two neutrons and a proton or vice versa. In contrast, the three-body interaction and clusters give a very small contribution to the SOS in ^7n in CVMC calculations. This suggests adding terms to the EDF that will produce a spin-orbit potential,

$$V_{\ell s}^{(n)}(r) = W_{\ell s}^{(2)} \frac{1}{r} \frac{d}{dr} [\rho(r) + \rho_n(r)] + W_{1,\ell s}^{(3)} \frac{1}{r} \frac{d}{dr} [\rho_n(r)\rho_p(r)] + W_{2,\ell s}^{(3)} \frac{1}{r} \frac{d}{dr} [\rho_p(r)]^2, \quad (7)$$

having separate two- and three-body contributions.The $[\rho_n(r)]^2$ term is omitted because three-neutron clusters seem to give negligible $V_{\ell s}^{(n)}(r)$. In neutron drops only the two-body $W_{\ell s}^{(2)}$ contributes, while in $N \sim Z$ nuclei, like ^{15}N, $\rho_n(r)\rho_p(r) \sim \rho_p(r)^2$ and the sum $W_{\ell s}^{(3)} = W_{1,\ell s}^{(3)} + W_{2,\ell s}^{(3)}$ is the only relevant new parameter.

With this modification to the spin-orbit interaction, and the FPS21 parametrization for the central interaction (including the gradient term for the neutron drops but not for ^{15}N), we can fit the spin-orbit splittings of ^{15}N and ^7n exactly, using the parameter values $W_{\ell s}^{(2)} = 61$ MeV fm^5 and $W_{\ell s}^{(3)} = 745$ MeV fm^8. The spin-orbit splittings in the eight closed-shell nuclei mentioned earlier are modified only slightly, a not unexpected result in view of their relatively small values of neutron excess.

In conclusion, we have made the first exact microscopic calculations of neutron drops in an external potential well. Our results suggest that the commonly used EDF's need modification in order to describe accurately neutron-rich nuclei. It appears that they predict neutron drops which are too dense and have too large a spin-orbit splitting. Our GFMC results also show that the CVMC using the improved Ψ_V', with two-neutron spin-orbit correlations gives fairly accurate results. We plan to use CVMC to calculate the properties of larger neutron drops. This, together with data from stable nuclei, will provide a larger database for fitting a Skyrme EDF for studies of stable nuclei, neutron-rich nuclei, and the surface of neutron stars.

We thank Dr. J. Dobaczewski and Dr. C. Gaarde for very useful advice. These calculations were made possible by generous grants of time on the IBM SP computer at the Mathematics and Computer Science Division, Argonne National Laboratory. The work of V.R.P., B.S.P., D.G.R., and A.S. is supported by the U.S. National Science Foundation via Grant No. PHY89-21025, that of S.C.P. by the U.S. Department of Energy, Nuclear Physics Division, under Contract No. W-31-109-ENG-38, and that of J.C. by the U.S. Department of Energy.

[1] C. J. Pethick, D. G. Ravenhall, and C. P. Lorenz, Nucl. Phys. **A584**, 675 (1995).
[2] K.-L. Kratz, J.-P. Bitouzet, F.-K. Thielemann, P. Möller, and B. Pfeiffer, Astrophys. J. **403**, 216 (1993). See also J. J. Cowan, F.-K. Thielemann, and J. W. Truran, Phys. Rep. **208**, 267 (1991).
[3] For a recent review of these topics, see C. J. Pethick and D. G. Ravenhall, Annu. Rev. Nucl. Part. Sci. **45**, 429 (1995).
[4] B. S. Pudliner, V. R. Pandharipande, J. Carlson, and R. B. Wiringa, Phys. Rev. Lett. **74**, 4396 (1995).
[5] S. C. Pieper, R. B. Wiringa, and V. R. Pandharipande, Phys. Rev. C **46**, 1741 (1992).
[6] S. C. Pieper and V. R. Pandharipande, Phys. Rev. Lett. **70**, 2541 (1993).
[7] R. B. Wiringa, V. G. J. Stoks, and R. Schiavilla, Phys. Rev. C **51**, 38 (1995).
[8] D. M. Ceperley and B. J. Alder, Phys. Rev. Lett. **45**, 566 (1980); M. A. Lee, K. E. Schmidt, M. H. Kalos, and G. V. Chester, Phys. Rev. Lett. **46**, 728 (1981).
[9] M. B. Leuschner *et al.*, Phys. Rev. C **49**, 955 (1994).
[10] D. Vautherin and D. M. Brink, Phys. Rev. C **5**, 626 (1972).
[11] D. G. Ravenhall, C. D. Bennett, and C. J. Pethick, Phys. Rev. Lett. **28**, 978 (1972).
[12] P. J. Siemens and V. R. Pandharipande, Nucl. Phys. **A173**, 561 (1971).
[13] H. Krivine, J. Treiner, and O. Bohigas, Nucl. Phys. **A336**, 155 (1980).
[14] V. R. Pandharipande and D. G. Ravenhall, in *Proceedings of a NATO Advanced Research Workshop on Nuclear Matter and Heavy Ion Collisions, Les Houches, 1989*, edited by M. Soyeur *et al.*, NATO ASI, Ser. B, Vol. **205** (Plenum, New York, 1989), p. 193.
[15] B. Friedman and V. R. Pandharipande, Nucl. Phys. **A361**, 502 (1981).
[16] J. Dobaczewski, I. Hamamoto, W. Nazarewicz, and J. A. Sheikh, Phys. Rev. Lett. **72**, 981 (1994).